Lawrence Berkeley Laboratory

UNIVERSITY OF CALIFORNIA

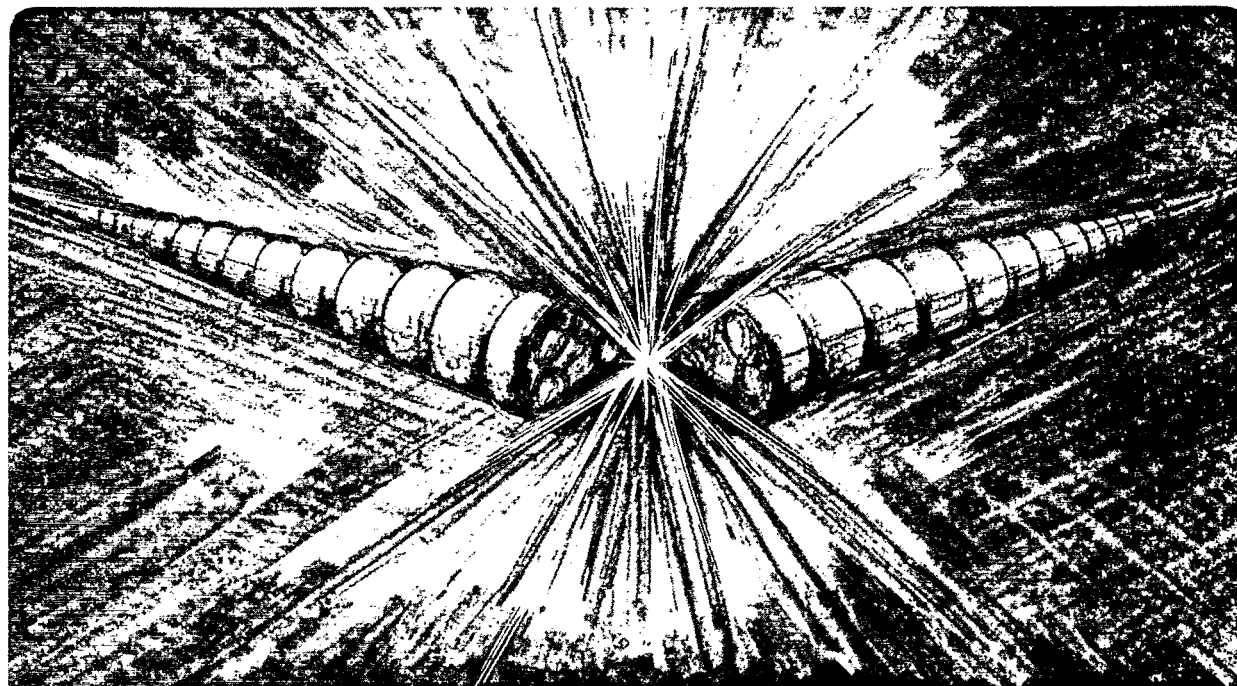## Accelerator & Fusion Research Division

RECEIVED
JUN 19 1996
OSTI

Soft X-Ray Magneto-Optic Kerr Rotation and Element-Specific Hysteresis Measurement

J.B. Kortright and M. Rice

March 1996

MASTER

DISCLAIMER

SOFT X-RAY MAGNETO-OPTIC KERR ROTATION AND ELEMENT-SPECIFIC HYSTERESIS MEASUREMENT*

J.B. Kortright and M. Rice

Center for X-ray Optics, Advanced Light Source
Lawrence Berkeley National Laboratory
University of California, Berkeley, California 94720

Soft X-Ray Magneto-Optic Kerr Rotation and Element-Specific Hysteresis Measurement

J.B. Kortright and M. Rice
Center for X-Ray Optics and Advanced Light Source
Lawrence Berkeley National Laboratory, Berkeley, CA 94720

Soft x-ray magneto-optic Kerr rotation has been measured using a continuously tunable multilayer linear polarizer in the beam reflected from samples in applied magnetic fields. Like magnetic circular dichroism, Kerr rotation in the soft x-ray can be element-specific and much larger than in the visible spectral range when the photon energy is tuned near atomic core resonances. Thus sensitive element-specific hysteresis measurements are possible with this technique. Examples showing large Kerr rotation from an Fe film and element-specific hysteresis loops of the Fe and Cr in an Fe/Cr multilayer demonstrate these new capabilities. Some consequences of the strong anomalous dispersion near the Fe $L_{2,3}$ edges to the Kerr rotation measurement are discussed.

Keywords: soft x-ray, Kerr magneto-optic effect, magneto-optic rotation, hysteresis measurement

I. INTRODUCTION

Magneto-optic effects result from the differential interaction of left and right circularly polarized radiation with the net electronic angular momentum of samples. Because linear polarization is a coherent superposition left and right circular polarization, both linear and circular polarization are useful in studying magneto-optical effects, and two very direct methods of observing them utilize incident beams having these different polarization forms. The differential absorption of left and right circular polarization is magnetic circular dichroism (MCD). The differential refraction of left and right circular polarization is not easily observed using circular polarization, but does produce magneto-optic rotation (MOR) of the plane of incident linear polarization that is easily observed with a linear polarizer in the transmitted or reflected beam. Magneto-optic effects were first observed in the visible as rotation of the plane of linearly polarized light on transmission through (Faraday, 1845) and reflection from (Kerr, 1876) samples in magnetic fields. In the visible range, a rich variety of magneto-optic effects have long been used to characterize magnetic materials [1], and the magneto-optic Kerr effect (MOKE) has been developed into a sensitive in situ probe of ultrathin magnetic films and interfaces [2].

In the last decade or so, magneto-optical studies of many types have been extended into the x-ray range. Resonant x-ray magneto-optic effects are largest when the photon energy is tuned near core levels from which dipole transitions couple initial core states to final magnetic states. The extreme ultraviolet and soft x-ray range extending from roughly 50 to 1500 eV contains core levels from which such dipole transitions can originate for nearly all magnetic elements, and hence provides a rich spectral field for element-specific magneto-optic investigations. Soft x-ray MCD using total electron yield to monitor absorption was early to develop, requiring only circular polarization obtainable as out-of-plane bending magnet radiation and total electron yield detection [3-5]. Together with theoretical sum rules [6-8], MCD spectroscopy is under investigation as a tool for determining spin and orbital atomic moments [9,10]. Magneto-optic effects detected in the reflected intensity have been observed using circular polarization [11,12]. These techniques measure a signal that is influenced both by refractive and absorptive effects, and in this sense are less direct than MCD and MOR techniques that measure the absorptive and refractive

response separately. Tunable linear polarizers for the 50 - 1000 eV range, based on multilayer interference structures, have been developed recently, and allow the extension of MOR techniques into the soft x-ray range [13]. The spectroscopic dependence of Faraday rotation across the Fe $L_{2,3}$ edges has been measured along with MCD from the same sample [14], with analysis demonstrating that soft x-ray MCD and MOR are related as expected by the Kramers-Kronig dispersion relationship and are in this sense equivalent.

In addition to element-resolved magneto-optic spectroscopy for moment determination, element-resolved hysteresis loops are of interest to provide a more complete understanding of magnetization processes in complex multicomponent materials. Different x-ray techniques offer capability here, and MCD using fluorescence yield detection first demonstrated element-specific hysteresis loops in layered magnetic films [15,16]. In this paper we report on the extension of MOKE, in which magneto-optic rotation is measured, into the soft x-ray range for element-specific hysteresis loop measurement. Soft x-ray MOKE (XMOKE) at the Fe and Cr edges in single films and multilayers of these materials are easily measured using a tunable linear polarizer and bending magnet radiation on the orbit plane. We find that for an Fe film the observed rotation is orders of magnitude larger at photon energies near the L_3 edge than in the visible, because of the direct and exclusive coupling to the magnetic 3d states. Element-resolved hysteresis loops revealing the magnetization in the Fe and Cr in Fe/Cr multilayers demonstrate how XMOKE can provide new information not obtainable from conventional hysteresis measurements, in which the net or aggregate magnetization of the sample is measured.

II. EXPERIMENT

A spectroscopic polarimeter using a laterally graded multilayer as a tunable linear polarizer enables the extension of magneto-optic rotation techniques into the 50 - 1000 eV range. This polarimeter is described in detail in ref. 13. Multilayers are well-suited to act as linear polarizers over this spectral range, since their synthetic nature allows adjustment of the period to position the Bragg peak at 45°, yielding a high extinction ratio. Lateral grading of the multilayer period, coupled with translation of the optic along the gradient, provides continuous tunability over a useful range, spanning the $L_{2,3}$ edges of the 3d transition elements, for example. The high reflectivity of multilayers results from an interference or Bragg peak, the

3

width of which can be controlled to some extent by the choice of materials and number of periods constituting the multilayer. Multilayer Bragg peaks at 45° having width of order 1° or greater and peak reflectance of 0.01 or greater can be obtained in this spectral range. The peak width is important for two reasons in this experiment, both stemming from the need to keep the angular tolerances of the experiment small with respect to the multilayer angular bandpass. First, only radiation falling within the angular bandpass of the multilayer polarizer is detected in the measurement with efficiency. Thus this is a brightness-limited experiment. Second, the angular alignment and rotation tolerances of the polarizer rotation axis with respect the beam must also be small with respect the Bragg peak width in order to keep the incident radiation centered on the peak. For a 1 degree wide Bragg peak, we can safely set a 1 mrad angular tolerance for these considerations. An entrance aperture on the polarimeter, together with other apertures in beamlines, can limit the angular acceptance of the device to 1 mrad without significant loss of intensity, assuming a bright synchrotron source such as the 3rd generation Advanced Light Source (ALS). Vacuum components for positioning and rotating the polarizer with 1 mrad tolerances are available. Compared to multilayers, large d-spacing natural crystals generally have much narrower Bragg peaks that reduce these angular tolerances correspondingly, making these crystals more difficult to implement as rotating polarizers for the above reasons. Even so, natural crystals can yield tunable polarizers through incidence angle tuning, and may provide useful tunable polarizers at energies above the range of multilayers.

Measurements reported here were made on bending magnet beamline 6.3.2 at the ALS.[17]. The samples were held in a longitudinal Kerr (reflection) geometry on the axis of a solenoidal electro-magnet (Figure 1) which was positioned on the sample stage in the beamline reflectometer chamber. Magnet pole pieces with tapered apertures allow the x-ray beam to reflect off of the sample with up to a 5° incidence angle, and produce very uniform fields along the illuminated length of the sample. With 328 windings the uncooled electromagnet produces a peak field of 2.5 kOe at 20 amps, but can not be operated for extended periods at these currents because of heating. Hysteresis loops reported here were measured with peak currents of from 1 to 10 amps. The polarimeter was bolted onto the downstream port of the reflectometer chamber and positioned to accept a beam reflected off of the sample at 1-2° incidence angle. The

polarimeter optical axis is easily aligned in the reflected beam by first translating its entrance aperture to maximize the transmitted flux and then adjusting two orthogonal tilts to align the rotation axis of the polarizer with the beam. This is accomplished using energy scans to determine the position of the multilayer Bragg peak at four azimuthal angles of the polarizer separated by 90°, and then adjusting the tilts to bring these four measured peaks into coincidence. Before performing XMOKE measurements, a Si wafer sample was placed in the magnet to reflect the beam with minimal change in polarization. Polarizer scans over 360° in azimuthal angle yield the degree of linear polarization [18], and in conjunction with adjustment of slits defining the vertical acceptance of the beamline were used to select an on-orbit portion of the bending magnet radiation having 0.97 to 0.98 degree of linear polarization.

Both the multilayer polarizers and the magnetic films and multilayers used in these experiments were deposited by magnetron sputtering. Substrates were oxidized Si wafers with no temperature control. The multilayer polarizers consist of W/B_4C multilayers having nominal d-spacing of 12.4 Å and 15.3 Å for use near the Fe and Cr L_3 edges, respectively. Each of these multilayers was laterally graded to yield a tunability range of roughly 10% centered around the L_3 edges. The Fe film reported on here was 470 Å thick and was capped with a SiC layer 15 Å thick to prevent oxidation. The Fe/Cr multilayer consisted of 40 periods each with a 20 Å thick Fe layer and a 19 Å thick Cr layer in a polycrystalline structure with (110) texture.

III. RESULTS

Measuring Kerr rotation at grazing incidence angles and near strong absorption resonances has important implications for the intensity of the signal and the magnitude of the observed rotation, which derive both from the nature of the anomalous dispersion near absorption edges in general and from the Kramers-Kronig transformation relating the absorptive (MCD) and refractive (MOR) magneto-optic responses. The reflection (Kerr) case is somewhat more complicated than the transmission (Faraday) case. In transmission the amount of material contributing to the magneto-optical effects is well-defined and constant with hv, while in reflection the penetration depth and hence the effective sample volume can

change rapidly with energy near core edges. The implications of these resonant effects in the reflection case are considered briefly below, and will be discussed in more detail in a separate paper.

Figure 2 partially demonstrates these implications for the case of the 470 Å thick Fe film onto which radiation is incident at 1.9° from grazing. Figure 2a shows the measured spectral reflectivity from the Fe film across the Fe $L_{2,3}$ edges, while Figure 2b shows the absorption measured by total electron yield across the same range. Each of these curves is free from magneto-optic effects, and hence represent standard anomalous dispersion effects relating $\delta(h\nu)$ and $\beta(h\nu)$, the real and imaginary corrections to unity in the complex refractive index $n(h\nu) = 1 - \delta(h\nu) - i\cdot\beta(h\nu)$. In the absorption spectrum the L_3 and L_2 white lines are clearly evident at 707 and 720 eV, respectively. The reflectivity profile across these edges shows strong resonant features with distinctly different shapes than the absorption spectrum.

Anomalous dispersion, independent of resonant magneto-optical effects, is extremely large at the Fe L_3 and L_2 edges, which are dominated by the large white lines in Fig. 2b resulting from dipole transitions from the $2p_{3/2}$ and $2p_{1/2}$ states to the empty 3d states. As shown in ref. 14, these absorption data can be normalized to yield $f''(h\nu)$, the imaginary part of the complex atomic scattering factor $f(h\nu) = Z + f'(h\nu) + i\cdot f''(h\nu)$. With $f''(h\nu)$, the Kramers-Kronig dispersion relation yields $f'(h\nu)$. δ and β are then obtained from f' and f'' via standard expressions [19]. For Fe, the negative resonance in f' just below the L_3 white line exceeds 26 electrons over a significant energy range, causing δ to become negative and the real part of the refractive index to become greater than unity. In this range where $1 - \delta > 1$, total external reflection no longer occurs, and the reflectivity falls, as seen in Fig. 2a. This decrease in reflectivity lowers the signal level available for measuring MOR, and simultaneously is accompanied by a significant increase in penetration depth in this region that increases the sample volume contributing to the Kerr rotation. In this region of decreased reflectance an oscillation in the reflectivity results from the interference of reflections from the top and bottom of the film, indicating a penetration depth comparable to the film thickness. Outside of the reflectance minimum below the L_3 white line these interference oscillations are not observed, indicating a penetration depth much less than the film thickness. At this 1.9° grazing incidence angle the penetration depth is less than 20 Å when tuned to the L_3 white line peak. Thus the experimenter can vary the penetration depth significantly at constant grazing incidence angle through these large anomalous

dispersion effects, with accompanying changes in reflected intensity. Note that MCD hysteresis techniques have necessarily limited sampling depths because the MCD signal is largest at the white line peak precisely where the absorption of the incident radiation is maximum. At the peak of the L_3 line $\beta \cong 0.006$, yielding a penetration depth for normal incidence of $\lambda/(4\pi\beta) = 233$ Å. Thus the largest penetration depth possible when tuned to the peak of the L_3 line, i.e., that at normal incidence, is less than the penetration depth obtained at 1.9° from grazing when the photon energy is tuned just several eV below the white line.

The magneto-optical absorptive (MCD) and refractive (MOR) response are related by the same Kramers-Kronig dispersion relation as are f'' and f' [14]. The MCD signal, $\beta_{left} - \beta_{right}$, shows peaks at the L_3 and L_2 white lines, with differing signs. Away from the white lines the MCD signal approaches zero. Consequently the MOR signal, $\delta_{left} - \delta_{right}$, undergoes a characteristic bipolar resonance at each line, with a significant non-zero value extending below the L_3 white line in the region where the MCD signal is essentially zero. This non-zero value of $\delta_{left} - \delta_{right}$ below the L_3 line, together with the significantly increased penetration depth below this line, imply that XMOKE hysteresis studies can be carried out at energies below the peak in $\delta_{left} - \delta_{right}$, which falls on the leading edge of the white line. Thus XMOKE hysteresis measurements can be made with varying depth sensitivity by tuning of photon energy below the edge.

Large magneto-optical rotation on reflection from this Fe film is seen in Figure 3, which shows polarizer azimuthal scans made with fixed 120 Oersted applied field saturating the magnetization parallel and antiparallel to the beam direction. For this measurement the photon energy was 5 eV below the L_3 white line which is well into the region of reduced reflectance and increased penetration. The observed rotation under these conditions is +/- 9.8° from the plane of the incident polarization. For Fe in the visible, longitudinal Kerr rotations are of order 0.1° depending on incidence angle and wavelength [20]. Thus the resonant XMOKE rotation can be at least 2 orders of magnitude greater than the comparable signal in the visible.

Element-specific hysteresis loops of the Fe and Cr magnetization behavior in an Fe/Cr multilayer are shown in Figure 4. The Fe/Cr multilayer system is of interest for its oscillatory Fe-Fe interlayer coupling and related large magneto-resistance [21]. The hysteresis loops in Fig. 4 were obtained with

7

photon energy tuned to 2.0 and 2.6 eV below the peaks in the L_3 white lines of Fe and Cr, respectively. The resonant nature of these x-ray magneto-optic effects means that tuning below the different elements L_3 edge yields responses just from that element. In each case the incidence angle was $2°$, and the azimuthal angle of the polarizer was fixed at 5° from the crossed position. Varying the applied field produced reflected intensity variations from the polarizer which were normalized to a rotation angle scale using the known shape of the rotating polarizer scan. Each data point corresponds to less than one second of signal integration time, with the complete loops requiring roughly 10 minutes to acquire. The strong spectroscopic dependence of the reflectance and penetration depth noted above for the Fe film are somewhat less pronounced for multilayer films, since the optical properties are not dominated by a single element. However photon energy is still an important parameter in determining both the reflectance and the magnitude of rotation for multicomponent samples, both homogeneous and inhomogeneous.

The individual hysteresis loops of just the Fe and Cr in the multilayer reveal several details of the magnetization process not obtainable from a standard hysteresis measurement, whose signal would represent the net or aggregate magnetic response of the sample. First, at least part of the Cr layers exhibit a significant magnetic moment, which is of interest since by itself Cr is antiferromagnetic with no net moment. Second, the Cr moment is oriented in the opposite direction to the Fe moment, since the two loops have the opposite sense. Third, both Fe and Cr loops show a coercive component closing near +/- 50 Oe, but only the Fe loop shows a reversible increase in magnetization as the field increases before saturating at fields above 1 kOersted. One possible model to explain these element-specific observations assumes an intermixed ferrimagnetic interface region in which Fe and Cr moments have opposite orientations. In this model the intermixing of Fe and Cr at the interfaces would account for the observed net Cr moment. Further experiments are underway to understand the element-specific responses in these relatively disordered, polycrystalline Fe/Cr samples, and to compare the responses in these systems with those from homogeneous alloys and more perfect, epitaxial multilayer samples. It is clear that these element-resolved XMOKE hysteresis measurements offer a wealth of new information that will further our understanding of magnetism in heterogeneous and homogeneous multicomponent materials.

IV. SUMMARY

Continuously tunable multilayer polarizers are well-suited to extend magneto-optic rotation techniques into the 50 - 1000 eV range that contains relevant core levels of most elements of interest in magnetism. While soft x-ray MOR techniques are capable of spectroscopic analysis including sum rule analysis to determine atomic moments, total electron yield soft x-ray MCD provides a simpler spectroscopy for samples in which electron detection is feasible. However, soft x-ray MOR offers new capabilities for element resolved hysteresis measurement in both the transmission and reflection geometry. The Kramers-Kronig dispersion relationship relating the real and imaginary parts of the optical constants, both independent of and specifically containing the magneto-optical response, have important spectroscopic implications for XMOKE measurements. In particular they show that working below the dominant L_3 white line of 3d transition metals can enhance the penetration depth to a value greater than that obtainable using fluorescence yield MCD techniques. For an Fe film the XMOKE rotation is at least two orders greater than in the visible range, and this large effect implies that XMOKE can provide more sensitivity than visible MOKE, assuming the x-ray measurement is not limited by photon flux. The separate magnetic response of Fe and Cr in Fe/Cr multilayers reveals features that are impossible to observe with standard hysteresis techniques and that will clearly be useful in understanding magnetism in this and related multilayer systems. Together these features imply that soft x-ray magneto-optic rotation techniques can play an important role in furthering our understanding of magnetism in multicomponent magnetic materials.

V. ACKNOWLEDGMENTS

VI. REFERENCES

1. M.J. Freiser, IEEE Trans. Magn. **MAG-4**, 152 (1968).

2. S.D. Bader, J. Magn. Mang. Mater. **100**, 440 (1991).

3. C.T. Chen, F. Sette, and S. Modesti, Phys. Rev. B **42**, 7262 (1990).

4. J.G. Tobin, G.D. Waddill, and D.P. Pappas, Phys. Rev. Lett. **68**, 3642 (1992).

5. Y. Wu, J. Stohr, B.D. Hermsmeier, M.G. Samant, and D. Weller, Phys. Rev. Lett. **69**, 2307 (1992).

6. B.T. Thole, P. Carra, F. Sette, and G. van der Laan, Phys. Rev. Lett. **68**, 1943 (1992).

7. P. Carra, B.T. Thole, M. Altarelli, and X. Wang, Phys. Rev. Lett. **70**, 694 (1993).

8. J. Stohr and H. Konig. Phys. Rev. Lett. **75**, 3748 (1995).

9. D. Weller, Y. Wu, J. Stohr. M.G. Samant. B.D. Hermsmeier, and C. Chappert, Phys. Rev. B **49**, 12888 (1994).

10. D. Weller, J. Stohr, R. Nakajima, A. Carl, M.G. Samant, C. Chappert, R. Megy, P. Beauvillain, P. Veillet, and G.A. Held, Phys. Rev. Lett. **75**, 3752 (1995).

11. C. Kao, J.B. Hastings, E.D. Johnson, D.P. Siddons, G.C. Smith, and G.A. Prinz, Phys. Rev. Lett. **65**, 373 (1990).

12. J.M. Tonnerre, L. Seve, D. Raoux, G. Soullie, B. Rodmacq, and P. Wolfers, Phys. Rev. Lett. **75**, 740 (1995).

13. J.B. Kortright, M. Rice, and K. Franck, Rev. Sci. Instrum. **66**, 1567 (1995).

14. J.B. Kortright, M. Rice, and R. Carr, Phys. Rev. B **51**, 10240 (1995).

15. C.T. Chen Y.U. Idzerda, H.-J. Lin, G. Meigs, A. Chaiken, G.A. Prinz, and G.H. Ho, Phys. Rev. B **48**, 642 (1993).

16. V. Chakarian, Y.U. Idzerda, G. Meigs, E.E. Chaban, J.-H. Park, and C.T. Chen, Appl. Phys. Lett **66**, 3368 (1995).

17. J.H. Underwood, E.M. Gullikson, M. Koike, P.J. Batson, P.E. Denham, K.D. Franck, R.E. Tackaberry, and W.F. Steele, these proceedings.

18. J.B. Kortright, M. Rice, Z. Hussain. H.A. Padmore, A. Adamson, W.R.A. Huff, A.T. Young, E.J. Moler, S.A. Kellar, R.X. Ynzunza, F.J. Palomares, H. Daimon, E.D. Tober, and C.S. Fadley, these proceedings.

19. R.W. James, *The Optical Principles of the Diffraction of X-rays*, (Ox Bow, Woodbridge, CT, 1982) Chaps. 2-4. The expression in ref. 14 expressing δ in terms of $Z + f'$ is missing the plus sign between these last two quantities.

20. see, for example, *International Critical Tables* (McGraw-Hill, New York, 1929) Vol. VI, p. 435.

21. M.N. Baibich, J.M. Broto, A. Fert, F. Nguyen van Dau, F. Petroff. P. Etienne, G. Creuzet, A. Friederich, and J. Chazelas, Phys. Rev. Lett. **61**, 2472 (1988).

Figure 1. Soleniodal electromagnet housing the sample in longitudinal Kerr geometry is shown. Conical holes in the pole pieces allow the x-ray beam to enter and exit the magnet at incidence angles up to 5 degrees.

Figure 2. (a) shows the spectral dependence of the reflectance from a 470 Å thick Fe film capped with SiC with a 1.9° incidence angle measured with a detector having no polarization sensitivity. (b) shows the total electron yield from the same sample with radiation incident near normal incidence, showing the L_3 and L_2 white lines at 707 and 720 eV, respectively. Each measurement was made with linearly polarized incident radiation, and hence is free from magneto-optic effects.

Figure 3. Polarizer scans showing directly the rotation of the plane of linear polarization incident at 1.9° from a 470 Å thick Fe film. The two polarizer scans shown were made with a positive and negative 120 Oersted applied field causing the Fe magnetization to saturate parallel and antiparallel to the beam directions. The photon energy is 702.0 eV, or 5 eV below the white line at the L_3 edge. The +/- 9.8° rotation is several orders greater than that observed from Fe in the visible.

Figure 4. Element-specific XMOKE hysteresis loops of just the Fe and Cr in Fe(20Å)/Cr(19Å) multilayer are shown in (a) and (b), respectively. Element-specificity is obtained by tuning photon energy just below the Fe and Cr L_3 white line in each case. The two hysteresis loops show both common and different features revealing the magnetization of each element of the multilayer. A standard hysteresis measurement would sense the net response of both elements, and would thus provide less information.
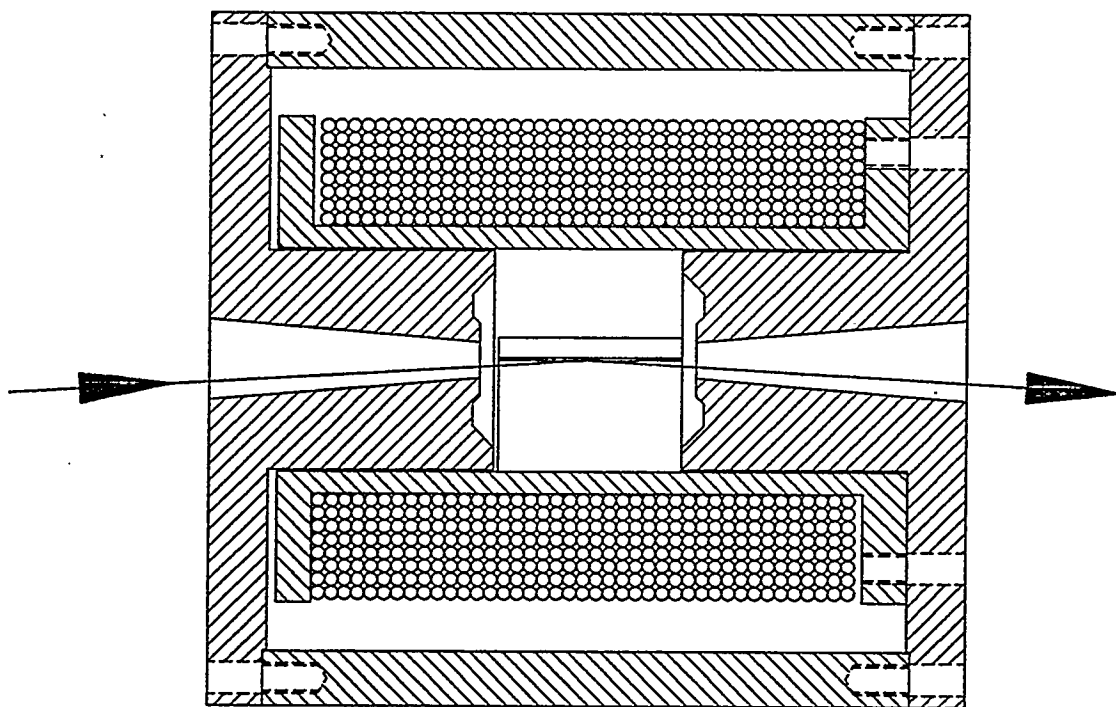
Figure 1
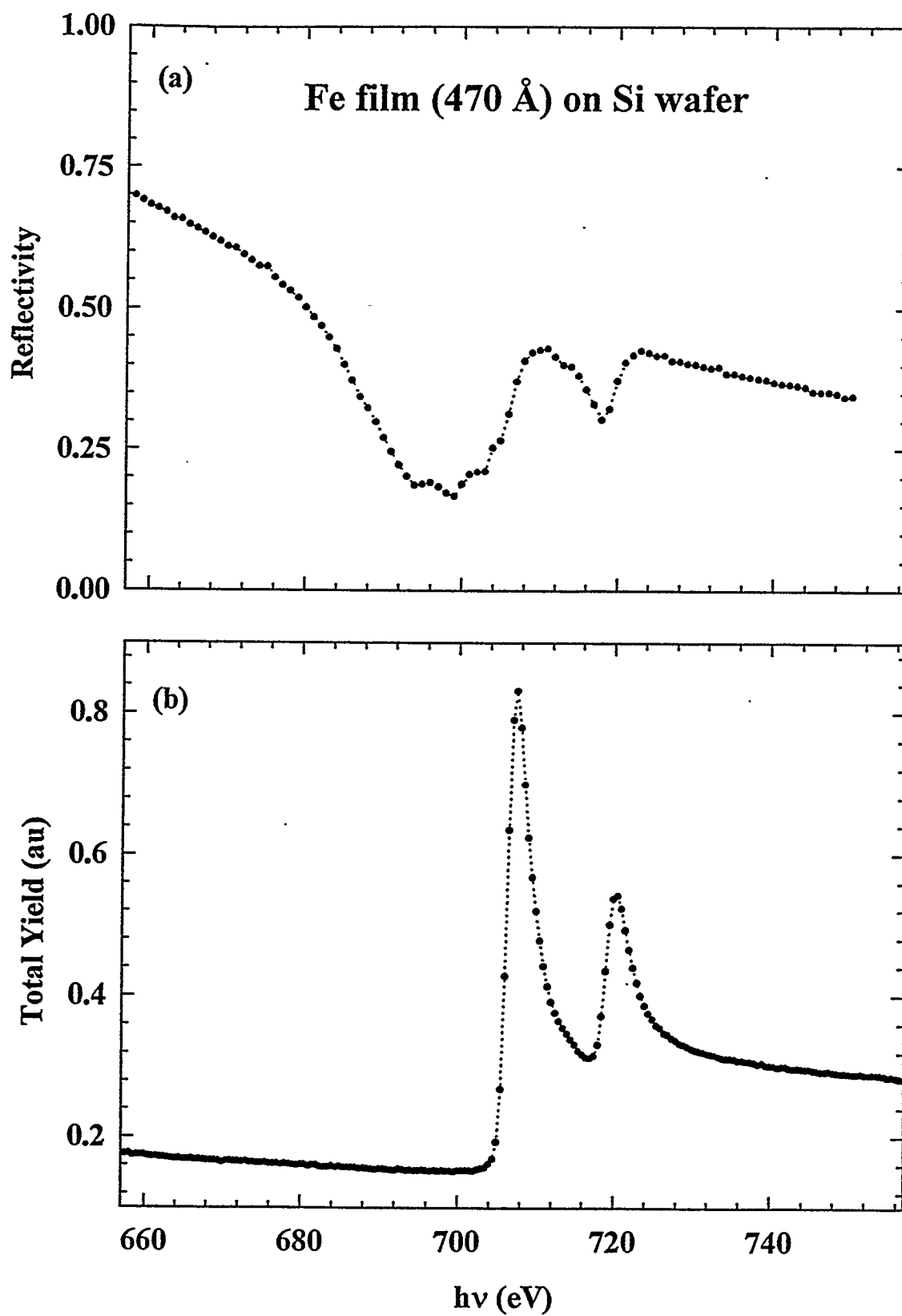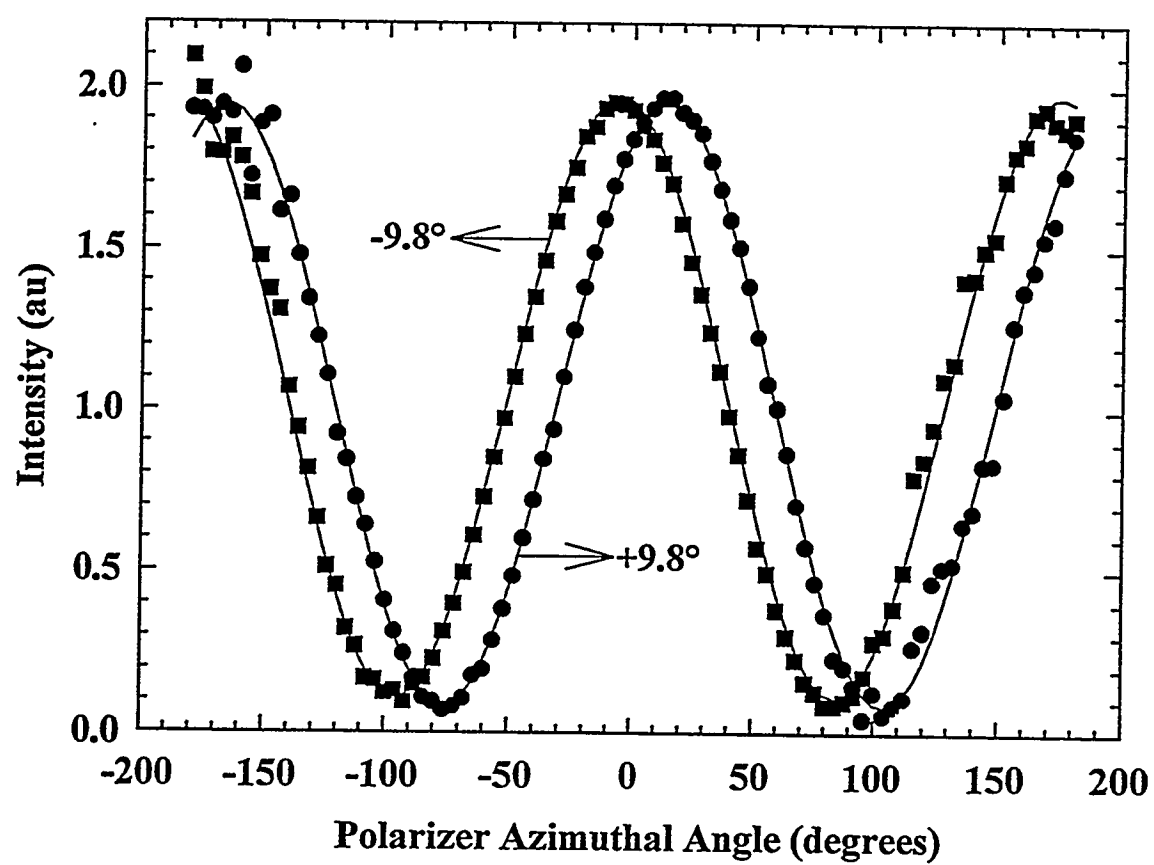
(a) Fe film (470 Å) on Si wafer
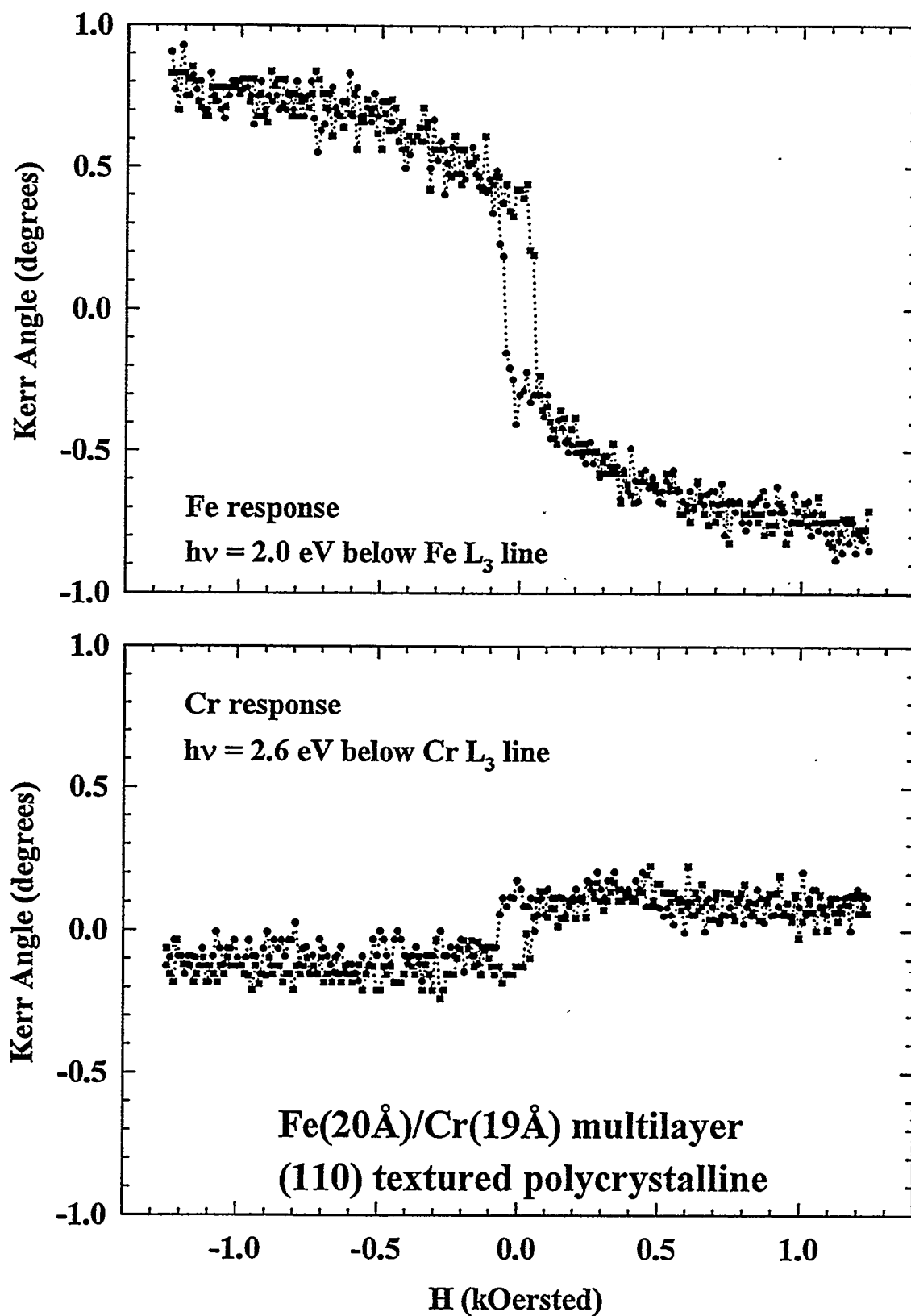
(b)

Figure 2

Figure 3

Figure 4

LAWRENCE BERKELEY NATIONAL LABORATORY
UNIVERSITY OF CALIFORNIA
TECHNICAL & ELECTRONIC INFORMATION DEPARTMENT
BERKELEY, CALIFORNIA 94720